John von Neumann Institute for Computing



Phase Transitions in Macromolecular Systems

Marcus Müller, Wolfgang Paul, and Kurt Binder

published in

NIC Symposium 2006 ,
G. Münster, D. Wolf, M. Kremer (Editors),
John von Neumann Institute for Computing, Jülich,
NIC Series, Vol. **32**, ISBN 3-00-017351-X, pp. 261-268, 2006.

© 2006 by John von Neumann Institute for Computing
Permission to make digital or hard copies of portions of this work for personal or classroom use is granted provided that the copies are not made or distributed for profit or commercial advantage and that copies bear this notice and the full citation on the first page. To copy otherwise requires prior specific permission by the publisher mentioned above.

http://www.fz-juelich.de/nic-series/volume32

Phase Transitions in Macromolecular Systems

Marcus Müller[1], Wolfgang Paul[2], and Kurt Binder[2]

[1] Institut für Theoretische Physik
Georg August-Universität, 37077 Göttingen, Germany
E-mail: mmueller@theorie.physik.uni-goettingen.de

[2] Institut für Physik, WA331
Johannes Gutenberg-Universität, 55099 Mainz, Germany

A new simulation method to study equilibrium properties and diffusive ordering kinetics in multicomponent polymer systems is discussed. Selected results for spinodal decomposition in symmetric binary polymer blends, solvent evaporation from thin polymer films and the order of diblock copolymer materials on nanopatterned surfaces are presented.

1 Introduction

Multi-component polymeric "alloys" are industrially and technologically omnipresent. In general, blending of different polymer species can reduce cost, improve processibility, provide synergy between components, allow for recycling, and improve overall properties. If one takes a binary blend of immiscible or partially miscible homopolymers, the blend may appear homogeneous on the length scale of centimeters, but it will consists of domains of μmeter size. The morphology of the phase separated material depends on the kinetics of phase separation. In this fine dispersion interfaces between the coexisting phases dictate many of the materials properties. In systems where the different components are chemically bonded together, i.e., a diblock copolymer, formation of macroscopic domains is impossible and the system forms domains on the size of the molecular extension, i.e., several tens of nanometers. If one could achieve defect-free ordering over macroscopic areas these materials would find applications in semiconductor industry or as filtration devices.

Properties on the length scales of molecular extension are universal, i.e. they depend on the chemical structure only via a small number of coarse-grained parameters: The molecular extension, R_e, sets the length scale. The incompatibility, χN, between different molecules sets the energy scale where χ is the Flory-Huggins parameter and N the molecular weight. The invariant degree of polymerization, $\bar{\mathcal{N}} \equiv (\rho R_e^3/N)^2$ where ρ denotes the monomer density, determines the strength of fluctuation effects[1].

In the SCF theory a system of interacting molecules is replaced by that of a single molecule in an external field which, in turn, depends on the local densities. This external external field mimic the interactions of the molecule with its neighbors. In the limit of large $\bar{\mathcal{N}}$ one molecule has interactions with $\mathcal{O}(\sqrt{\bar{\mathcal{N}}})$ neighboring molecules and replacing these fluctuating fields by their thermal averages (i.e., the mean field approximation) becomes accurate. While the SCF theory has found ample successful applications it is numerically difficult to study complex three-dimensional geometries, to incorporate details of the molecular architecture beyond the Gaussian chain model and to extend the theory to the description of the kinetics of phase separation and ordering[1,2].

Our report is arranged as follows: In the next section, we describe a computational method – single chain in mean field simulations – that is able to partially overcome the difficulties mentioned above. Then, we present selected applications to the kinetics of phase

separation and ordering as well as the self-assembly of diblock-copolymers on patterned substrates. The paper closes with a brief outlook.

2 Single Chain in Mean Field (SCMF) Simulations

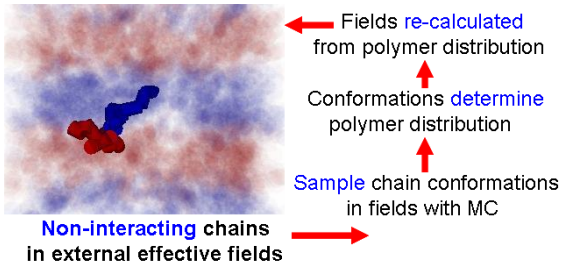


Figure 1. Sketch of Single Chain in Mean Field (SCMF) simulations.

We consider a large ensemble of independent chains in an external field. The chains are described by a coarse-grained polymer model. In our applications we have utilized a simple bead-spring model comprising N beads. The single chain probability distribution takes the form of a discretized Edwards-Hamiltonian augmented by a bending potential[3]:

$$\mathcal{P}_{A,\alpha}[\{\mathbf{r}_\alpha\}] \sim \Pi_{i=1}^{N-1} e^{-\frac{3(\mathbf{r}_{\alpha,i}-\mathbf{r}_{\alpha,i+1})^2}{2b^2}} \Pi_{i=1}^{N-2} e^{f_{\text{stiff}}(\mathbf{r}_{\alpha,i}-\mathbf{r}_{\alpha,i+1})(\mathbf{r}_{\alpha,i+1}-\mathbf{r}_{\alpha,i+2})} \quad (1)$$

The simulation method is sketched in Fig. 1[3]: Chain conformations are updated in the external fields via a standard Monte Carlo scheme utilizing local random displacements of the beads. After a short, predetermined number of Monte Carlo steps, the spatial density distribution created by the large ensemble of independent molecules is determined and the relation of the SCF theory between density and field is employed to calculate the new, external fields. Then, the process is iterated.

- This particle-based simulation method utilizes coarse-grained polymer models (e.g., bead-spring model with bond angle potential) and is not limited to the Gaussian chain model of the SCF theory. The use of explicit molecular conformations allows details of the chain architecture to be incorporated (e.g., stiffness along the backbone or branching).

- The density (and external fields) accurately mimic the instantaneous chain conformations. SCMF simulations converge to a solution of the equilibrium SCF theory in the limit of an infinitely large ensemble, $\bar{\mathcal{N}} \to \infty$. Numerical calculations for binary blends and diblock copolymers demonstrate that this simulation scheme can describe composition fluctuations (cf. Fig. 2) if the fields are updated frequently. This finding has been corroborated by approximate but analytical techniques.

- The explicit propagation of the chain conformations avoids the need of an Onsager coefficient and intramolecular correlations (that give rise to a non-local Onsager coefficient in field-theoretic schemes) are taken into due account.

- Propagating the explicit chain conformations in time we are able to investigate blends with strong dynamic asymmetries (e.g., where one component vitrifies during the phase separation process).

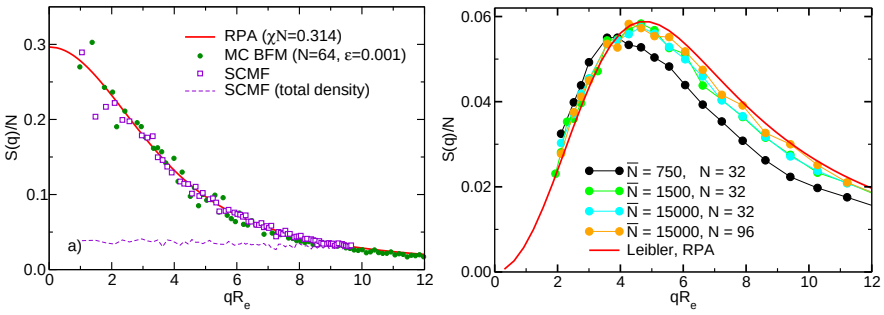


Figure 2. (a) Equilibrium composition fluctuations of a symmetric binary polymer blend at $\chi N = 0.314$ as obtained from Random Phase Approximation, MC simulations of the bond fluctuation model, and SCMF simulations. The horizontal dashed line also depicts the structure factor of the total density in the SCMF simulations which utilize a small but finite compressibility. From Ref. 3. (b) Equilibrium composition fluctuations of a symmetric diblock copolymer at $\chi N = 2$ as obtained from SCMF simulations and Random Phase Approximation for a system of linear dimension, $L = 3R_e$. To achieve an invariant degree of polymerization of $\bar{\mathcal{N}} = 15000$ (which corresponds to an intermediate molecular weight) in a typical bead spring model ($\rho = 0.83$) requires a large system of very long chains, i.e., 3400 chains each comprising $N = 3000$ beads. In the SCMF simulations we can reproduce these experimental values of $\bar{\mathcal{N}}$ simply by increasing the density rather than the chain discretization, N.

Additionally the scheme is computationally efficient, permits us to study large system sizes and it is suitable for parallel computers. To this end, we distribute the independent chain conformations evenly across the processors independent of their location in space. Each processors performs the Monte Carlo simulations for "its" molecules which are mutually independent but only interact with the external field. Each processors calculates the density of its molecules after the Monte Carlo simulation and the results are summed across the processors to construct the new external field for the next simulation. Typically we utilize between 8 and 64 processors on the IBM Regatta at the NIC, Jülich.

3 Applications

3.1 Spinodal Decomposition in Binary Polymer Blends

First we discuss the growth of composition fluctuations in a binary symmetric polymer blend in response to a temperature quench from the one-phase region, $\chi N = 0.314$ into the miscibility gap, $\chi N = 5$. Early stages of spinodal decomposition are characterized by an exponential growth of collective concentration fluctuations. The growth rate, $R(q)$, depends on the wavevector, q, the equilibrium thermodynamics of the mixture, and the dynamics of the molecules. The latter enter the field theoretical description via an Onsager coefficient which describes the relation between a gradient of the chemical (exchange) potential and the concomitant concentration current. Due to the extended shape of the

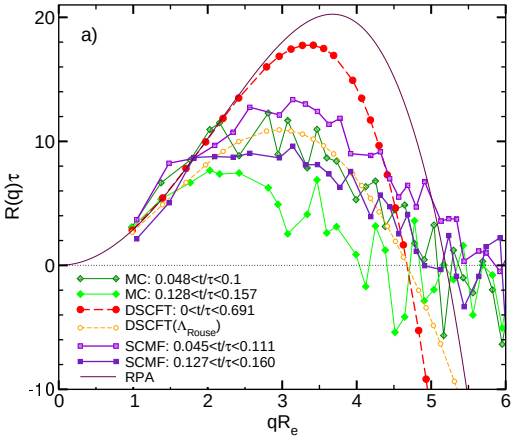


Figure 3. Growth rate, $R(q)\tau$, of the collective structure factor, $S(q) \sim \exp[R(q)t]$, as a function of the wavevector, q. Data from MC simulations of the bond fluctuation model at an early and intermediate time regime and the results from the dynamic SCF theory using a local and a Rouse-like Onsager coefficient are adapted from Ref. 2. The results of the SCMF simulations slightly overestimate the initial growth rate at large wavevectors, but capture the fastest growing mode, the decrease of the rate with time and do not predict negative rates (damping) at high wavevectors in agreement with the MC simulations. The prediction of the Random Phase Approximations is also included as thin solid line.

macromolecules the Onsager coefficient is non-local and explicit expressions exists for the homogeneous system[4]. The results from Monte Carlo simulations of the bond fluctuation model, dynamic SCF calculations calculations with a local Onsager coefficient and an Onsager coefficient for Rouse-dynamics, and the results of SCMF simulations are compared in Fig. 3. Clearly, a local Onsager coefficient fails to describe the simulation results, but dynamic SCF calculations using a non-local Onsager coefficient and SCMF simulations that do not utilize an Onsager coefficient but rather propagate the explicit chain conformations in time yield an improved description.

It is also instructive to compare the computational effort between the different schemes: For the MC simulations of 64 independent systems over the time interval 0.33τ a computational effort of 40 days on 64 processors of a CRAY T3E was needed. Using $7\times7\times7 = 343$ grid points in Fourier space the corresponding dynamic SCF calculations required about 25 days on a CRAY J90. The single chain mean field calculations of 64 independent systems, each with twice as many polymers than in the MC simulations and a spatial resolution of 4096 grid points, took 19 hours on a 32×2 node Beowulf cluster of Opteron (1.8GHz) processors.

While explicit analytical expression for the non-local Onsager coefficient exist for spatially homogeneous systems (appropriate, e.g., for the early stages of spinodal decomposition), no such expression exist at spatial inhomogeneities (e.g., interfaces or surfaces). Under those circumstances the chain conformations are distorted and the calculation of the Onsager coefficient amount to calculate intramolecular correlations which is computationally infeasible.

3.2 Solvent Evaporation from Thin Polymer Films

The kinetics of phase separation in the presence of strong spatial and dynamic inhomogeneities is explored in Fig. 4 where we compare SCMF simulations with Molecular Dynamics simulations of the evaporation of a volatile solvent from a thin polymer film. To match the SCMF simulations with the Molecular Dynamics simulations we utilized the single chain structure factor to adjust the bond length, b, and the chain stiffness, $f_{\rm stiff}$ in Eq. (1). The interactions were modelled via a virial expansion[5] and the coefficients were

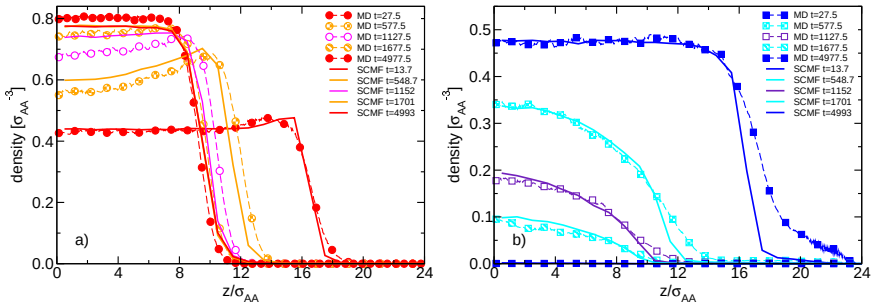


Figure 4. Polymer (a) and solvent (b) density, $\phi_A(\mathbf{r},t)$ and $\phi_B(\mathbf{r},t)$, as a function of time during the evaporation process as observed by MD simulations of a bead-necklace model and by SCMF simulations using a parameterization for the coexistence densities and segmental mobilities. All times are measured in units of Lennard-Jones time units. From Ref. 3.

adjusted to reproduce the phase equilibrium. The time scales were matched by comparing the self-diffusion constants in the bulk.

The time evolution as well as the details of the density profiles of polymer and solvent are quantitatively well predicted by SCMF simulations (cf. Fig. 3) even if interfaces are present. Upon evaporation of the solvent a dense polymer layer ("skin") builds up at the polymer-vapor interface at intermediate times. One advantage of the SCMF simulations is that we can control the mobility of the species without changing the equilibrium thermodynamics. Altering the mobilities, we obtain rather direct insight into the importance of the density dependence of the segmental dynamics, which is less straightforward to extract from simulations of the interacting multi-particle system. For instance, if we neglect the concentration dependence of the solvent mobility we do not find the formation of a skin.

3.3 Microphase Separation of Block Copolymers on Nanopatterned Substrates

We have used SCMF simulations to explore the self-assembly of copolymers and their mixtures with the corresponding homopolymers in nanopatterned substrates[6–8]. The self-assembly is dictated by an intricate interplay between interfacial interactions, breaking of translational symmetry, and structural frustration due to the incompatibility between the natural periodicity of the bulk structure and film thickness and the substrate pattern. Confinement and surface effects can result in morphologies that are absent in the bulk, e.g., surface reconstructions.

Fig. 5 shows the ordering of a lamellar-forming diblock on top of a stripe pattern. There is a slight mismatch between the bulk lamellar period, $L_0 = 1.786R_e$ at $\chi N =$ and the pattern period, $L_S = 1.7$. In the initial stage perfectly registered lamellae are formed at the substrate (substrate-directed ordering). The top (bulk) of the film segregates into microdomains later and they are not registered with the substrate pattern. Defects in the structure anneal not by lateral diffusion but the order of the registered lamellae propagates from the substrate to the top surface[6].

It is of interest to explore what geometrical patterns can be reproduced by diblock copolymer materials. Generally, only a small mismatch between the natural morphology of the diblock and the substrate pattern is permissible if defect-free registration and order

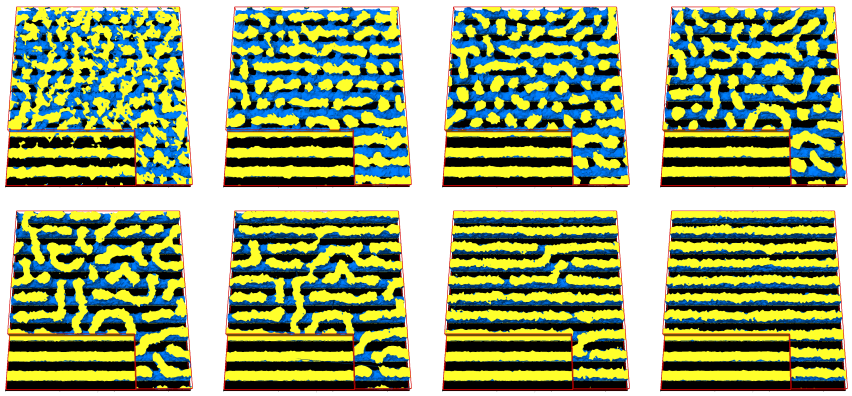


Figure 5. Snapshot images of the three dimensional behavior of diblock copolymers on chemically nanopatterned substrates. The lateral system size is $17R_e \approx 0.5\mu$m. The time increases from left to right and from top to bottom. One component has been removed from the image and blue surfaces represent the interface between the different components. In the lower left corner 75% of the film has been removed to reveal the near-substrate morphology. From Ref. 6.

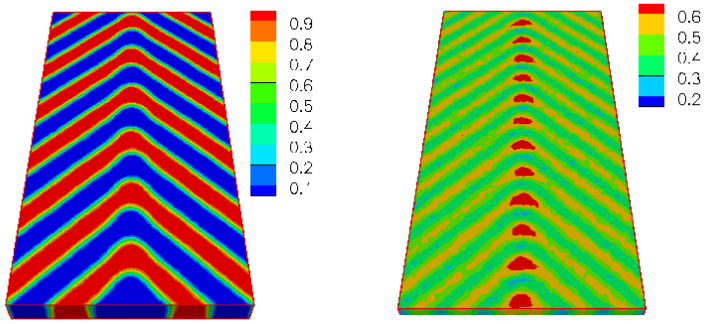


Figure 6. Three-dimensional contour plots of the composition (left) and the total homopolymer concentration (right) obtained from SCMF simulations. In the left panel the red and blue areas represent A- and B-rich domains, respectively. In the right panel, the periodic red areas are enriched alternatively in A and B homopolymers, whereas the blue stripes represent the domain interfaces that are depleted of homopolymers. From Ref. 7.

is required. Using blends of AB-diblock copolymers with the corresponding A- and B-homopolymers is an experimentally convenient way to adjust (enlarge) the periodicity and it also is crucial for replicating more complex patterns. This is illustrated in Fig. 6 where the ordering of a ternary blend on a nested array of bends is shown. The periodicity of the stripes matches the bulk lamellar spacing but the distance between the AB interfaces at the corners is larger. The homopolymers redistribute as to selectively swell the morphology at the corners resulting in defect free ordering. Note also the Ω-shape of the AB-interface at the corners which resembles domain shapes observed at grain boundaries in the bulk[7].

If one increases the mismatch between the length scale or the symmetry of the substrate pattern and the bulk morphology of the diblock the copolymers do no longer register with

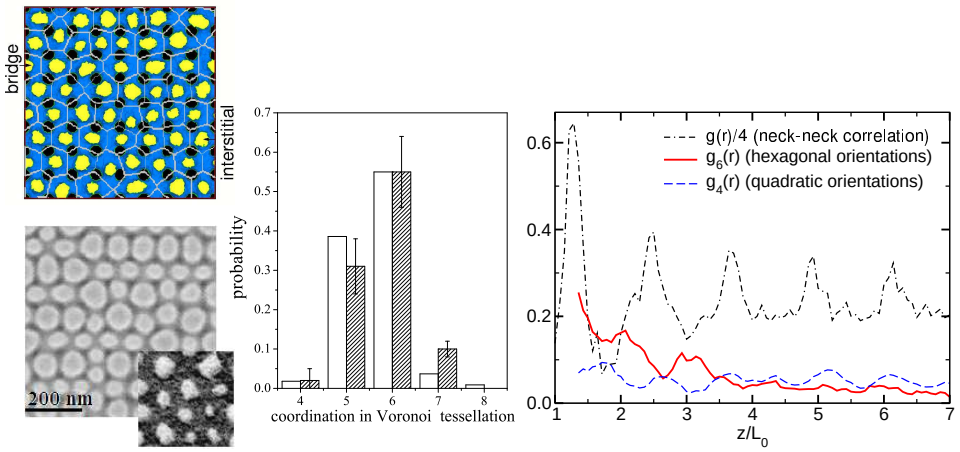


Figure 7. Morphology of a copolymer/homopolymer blend film of thickness $D_0 = 0.63L_0$ and lateral dimensions of $9.77L_0$ on a square array of spots. (top left) SCMF simulation showing only the top view of the PS-rich domains (white/yellow) and the interface between PS and PMMA (dark grey/blue). Regions on top of the spots are PMMA-rich (transparent) and one looks through to the substrate (black). The position between two PMMA-attracting spots of the substrate is denoted as "bridge", while the position at the center of a plaquette of four spots is denoted "interstitial". The Voronoi tessellation of the necks is indicated by thin white lines. (bottom left) SEM image of the composition at the film surface. The PS-domains are shown in light grey while PMMA-rich surface areas correspond to dark grey regions. Note that the PS-domains appear artificially larger in the SEM images so a more accurate view of the domain sizes is provided by an AFM phase image shown as an inset at the lower right corner. (middle) Probability distribution of the coordination (number of edges) of Voronoi cells (c.f. top left panel). The "errorbars" of experimental data (shown in grey) characterize the variance of results obtained by analyzing different SEM images of size $9.77L_0$. SCMF simulation results are shown as open bars. (right) Pair correlation of the necks and orientational correlation functions for hexagonal and square orientations extracted from large SEM images. From Ref. 8

the bulk pattern. This is illustrated in Fig. 7 which shows the disordered bicontinuous morphology of a lamellar-forming ternary blend on top of a surface pattern that consists of a square array of spots with center-to-center distance, $\lambda = 1.21L_0$, and radii, $R = 0.30L_0$.

Near the substrate the morphology replicates the substrate pattern and forms a quadratically perforated lamellar (QPL) sheet[8]. Necks of polystyrene (PS) connect to this QPL. The near-substrate morphology favors a square geometry of the necks while the packing of dense necks rather results in a hexagonal structure. This competition prevents the formation of long-range order and one observed in the SCMF simulations as well as in the experiments a disordered bicontinuous structure. The local geometry can be characterized by a Voronoi tessellation which reveals a substantial amount of 6-fold coordinated necks. The local hexagonal structure is also revealed by the orientational correlation function, g_6[9]

$$g_n(r) = \left\langle \left| \frac{1}{n} \sum_{\alpha \in \langle \mathrm{nn} \rangle_i} e^{in\phi_{\alpha i}} \frac{1}{n} \sum_{\beta \in \langle \mathrm{nn} \rangle_j} e^{-in\phi_{\beta j}} \right| \right\rangle \tag{2}$$

where α and β run over all nearest neighbors (nn) (as identified via the neck-neck-pair

correlation function) of the two necks i and j a distance r apart and $\phi_{\alpha i}$ is the angle of the vector between the center of the neck i and its neighbor α. Hexagonal correlations are strong but short-ranged while orientational correlations with $n = 4$ are weaker but longer-ranged and are mediated over long distances by the substrate pattern.

4 Concluding Remarks

Single chain in mean field simulations are a computationally efficient method to study the morphology of multi-component polymer systems on parallel computers. Nevertheless a careful investigation of the potential and limitations of the method is still required to clarify under which conditions fluctuations are correctly described and how to optimally choose the spatial discretization and updating frequency of the fields. Other interesting aspects consist in extending the dynamics to entangled systems by using the slithering snake algorithm (in addition to local random displacements) or to introduce a fine network of strings which do not influence the equilibrium behavior but are uncrossable and, thus, will lead to reptation-like motion.

Acknowledgments

It is a great pleasure to thank the John von Neumann Institute for Computing for a generous allocation of CPU time on the IBM Regatta and to acknowledge K. Daoulas, E.W. Edwards, P.F. Nealy, J.J. de Pablo, Y.J. Papakonstantopoulos, S.-M. Park, E. Reister, G.D. Smith, F. Schmid, and M. Stoykovich for fruitful and enjoyable collaboration. Financial support was provided by the Volkswagen foundation and the DFG und grant Mu 1674/3.

References

1. M. Müller and F. Schmid, Adv. Polym. Sci. **185**, 1 (2005).
2. E. Reister, M. Müller and K. Binder, Phys. Rev. **E 64**, 041804 (2001).
3. M. Müller and G.D. Grant, J. Polym. Sci. **B 43**, 934 (2005).
4. K. Binder, J. Chem. Phys. **79**, 6387 (1983).
5. K. Binder, M. Müller, P. Virnau, and L.G. Mac Dowell, Adv. Polym. Sci. **173**, 1 (2005).
6. E.W. Edwards, M.P. Stoykovich, M. Müller, H.H. Solak, J.J. de Pablo and P.F. Nealey, J. Polym. Sci. **B 43**, 3444 (2005).
7. M.P. Stoykovich, M. Müller, S.O. Kim, H.H. Solak, E.W. Edwards, J.J. de Pablo, and P.F. Nealey, Science **308**, 1442 (2005).
8. K.Ch. Daoulas, M. Müller, M.P. Stoykovich, S.-M. Park, Y.J. Papakonstantopoulos, J.J. de Pablo, and P.F. Nealey (submitted).
9. D.R. Nelson and B.I. Halperin, Phys. Rev. **B 19**, 2457 (1979).